JOURNAL OF COMPUTATIONAL PHYSICS 116, 123–134 (1995)

Smoothed Particle Hydrodynamics Stability Analysis*

J. W. SWEGLE

Solid and Structural Mechanics, Department 1562, Sandia National Laboratories, Albuquerque, New Mexico 87185

D. L. HICKS

Department of Mathematical Sciences, Michigan Technological University, Houghton, Michigan 49931

AND

S. W. ATTAWAY

Computational Mechanics and Visualization, Department 1425, Sandia National Laboratories, Albuquerque, New Mexico 87185

Received April 9, 1993; revised February 8, 1994

SPH (smoothed particle hydrodynamics) is a gridless Lagrangian technique which is appealing as a possible alternative to numerical techniques currently used to analyze large deformation events. Recent tests of the standard SPH method using the cubic B-spline kernel indicated the possibility of an instability in the tensile regime, even though no such difficulties were observed in compression. A von Neumann stability analysis of the SPH algorithm has been carried out which identifies the criterion for stability or instability in terms of the stress state and the second derivative of the kernel function. The analysis explains the observation that the method is unstable in tension while apparently stable in compression but shows that it is possible to construct kernel functions which are stable in tension and unstable in compression. The instability is shown to result from an effective stress with a negative modulus (imaginary sound speed) being produced by the interaction between the constitutive relation and the kernel function and is not caused by the numerical time integration algorithm. That is, changes in the effective stress act to amplify, rather than reduce, perturbations in the strain. The analysis and the stability criterion provide insight into possible methods for removing the instability.

1. INTRODUCTION

SPH (smoothed-particle hydrodynamics) [1–8] is a gridless Lagrangian technique which is appealing as a possible alternative to numerical techniques currently used to analyze high deformation events. While Eulerian techniques can easily handle the gross motions associated with the large deformations involved in such events, detailed analysis is difficult because of the lack of history and the smearing and spreading of information as the mass moves through the fixed-in-space Eulerian grid. Standard Langrangian techniques, although desirable due to their ability to keep accurate histories of the events associated with each Lagrangian element, are difficult to use because the material deformations are so large that the Lagrangian grid becomes severely distorted and the calculation breaks down. SPH offers a potential solution to these difficulties. However, SPH is a relatively new method, especially in applications involving solid materials capable of supporting deviatoric and tensile stresses. Thus, critical evaluations and tests are needed. This paper describes a stability analysis of the SPH equations; the need for this has been recognized for some time [3] and interest in the subject is increasing [9].

Tests of the standard SPH method indicate an instability in the tensile regime, even though the calculations appear to be stable in compression. The simplest example of a test calculation exhibiting the instability involves a body which is subjected to a uniform initial stress, either compressive or tensile. The positions of particles near the boundaries of the body are fixed to avoid wave propagation which relieves the initial stress. The calculations described below use the cubic B-spline kernel [8] and have all viscosities turned off in order to separate properties of the basic algorithm from effects due to artificial viscosity. Figure 1.1 shows the initial configuration for a two-dimensional calculation. A velocity perturbation of 10^{-10} km/s is applied to a single particle at the center of the body. If the stress is compressive, no change in the particle positions is detected, since at the initial perturbation velocity it would take 10^4 s for a particle to move a distance equal to the particle separation. However, if the stress is tensile, the result in Fig. 1.2 is obtained after only 100 μs. The magnitude of the effect is clear. The particles have clumped together and large voids have formed, seriously affecting the uniform density initially present in the

* This work was performed at Sandia National Laboratories and was supported by the U.S. Department of Energy under contract number DE-AC04-76DP00789.

0021-9991/95 $6.00

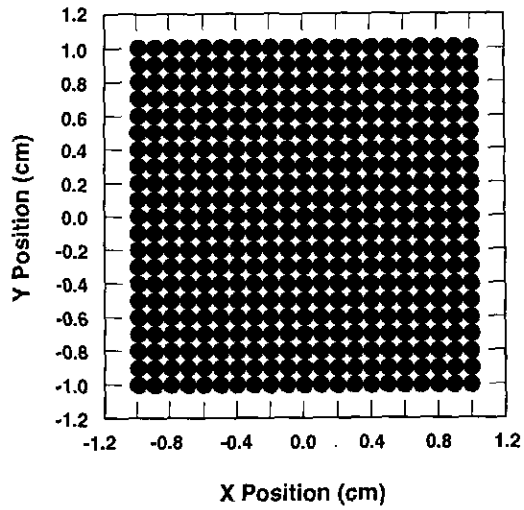

FIG. 1.1. Initial particle positions in 2D stability test.

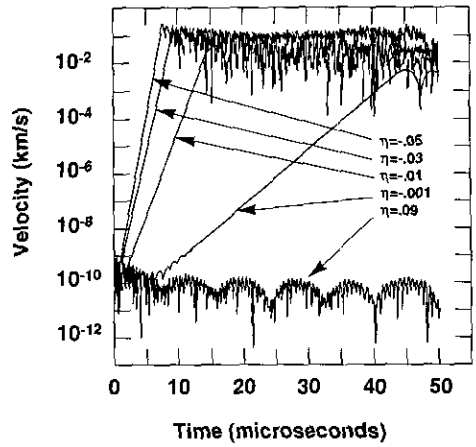

FIG. 1.3. Perturbation amplitude histories for various initial levels of volume strain, $\eta = 1 - \rho_i/\rho_{ref}$, where ρ_i is the initial density at which the calculation is started and ρ_{ref} is the reference density at which the stress in the material is zero. The stress, which for small strains is proportional to the strain, is compressive if the volume strain is positive, and tensile if the volume strain is negative.

calculation. Similar effects are seen whether test problems are run in one, two, or three dimensions. For example, results from a one-dimensional analogue of the above two-dimensional calculation are shown in Fig. 1.3, which is a plot of the velocity history of the perturbed particle for initial stresses corresponding to various initial volume strains. The large perturbations in particle positions such as illustrated in Fig. 1.2 are due to exponential growth of particle velocities, clearly indicating the presence of an instability. The velocity grows by many orders of magnitude for any level of tensile stress (negative volume strain), although the growth rate depends on the stress level. The velocity does not grow if the stress is compressive (positive volume strain). However, even in the unstable cases the exponential growth does not continue indefinitely, but eventually switches to a somewhat oscillatory motion. The instability thus results in particle clumping rather than complete blowup of the particle positions to infinity. Unfortunately, this artificial numerical clumping mimics physical processes of fracture and fragmentation in many situations, making the instability hard to detect.

The stability analysis provides a criterion for instability in terms of the stress state and the second derivative of the kernel function. It provides an explanation of the behavior seen in the figures, including the unusual property of apparent stability in compression coupled with instability in tension. It also explains the termination of the exponential growth phase after large enough levels of distortion have been reached.

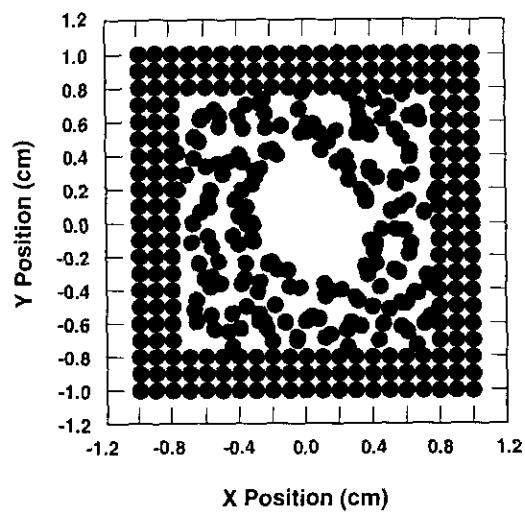

FIG. 1.2. Particle positions at 100 μs, showing the effect of the tensile instability.

2. SPH EQUATIONS

2.1. *Kernel Approximation*

Consideration of standard Lagrangian finite-difference techniques [10] shows that the major purpose of the spatial grid is to provide a basis for the construction of approximations to spatial derivatives. The smoothed particle technique involves replacing grid-based approximations with algorithms applicable to an arbitrary collection of interpolation points. The basis of the method is the kernel estimate [5],

$$f(x) \approx \sum_{J=1}^{N} \frac{m^J}{\rho^J} f(x^J) W(x - x^J, h), \tag{2.1}$$

where f is a vector function of the three-dimensional position vector x, m^J, and ρ^J are the mass and density at point J, and $W(x - x^J, h)$ is an interpolating kernel function with smoothing length h. The requirements that are usually placed on the kernel function [3] are (1) it reduces to the delta function,

$$\lim_{h\to 0} W(x, h) = \delta(x), \tag{2.2}$$

(2) it is normalized,

$$\int W(x, h)\, dx = 1, \tag{2.3}$$

and (3) it has compact support (is zero everywhere but on a finite domain),

$$W(x, h) = 0 \quad \text{for } |x| \geq 2h. \tag{2.4}$$

The approximation for spatial derivatives is obtained by taking the divergence of Eq. (2.1) with respect to x,

$$\nabla \cdot f(x) \approx \sum_{J=1}^{N} \frac{m^J}{\rho^J} f(x^J) \cdot \nabla W(x - x^J, h). \tag{2.5}$$

The above equations provide continuous approximations to a vector function and its divergence based on an arbitrary set of discrete interpolation points at which the function is known. No connectivity or spatial relation of the points is assumed.

2.2. *Conservation Laws*

The SPH method provides numerical solutions to initial-boundary value problems defined by the conservation laws of continuum mechanics plus constitutive relations for the materials involved. In the case in which the material description is energy-independent, the conservation laws to be solved express the conservation of mass

$$\frac{\dot{\rho}}{\rho} = -\nabla \cdot V = -(\nabla \cdot (\rho V) - V \cdot \nabla \rho)/\rho, \tag{2.6}$$

where v is the velocity vector and the superimposed dot on the density refers to the material time derivative, plus the conservation of momentum

$$\ddot{x} = \frac{1}{\rho} \nabla \cdot \sigma, \tag{2.7}$$

where $\ddot{x}$ is the acceleration and σ is the Cauchy stress tensor, taken as negative in compression. The kernel approximation is used for the spatial derivatives in these expressions. Various schemes exist for advancing the solution in time, but a simple centered-difference scheme, sometimes known as a leapfrog scheme, for the approximation of time derivatives will result in a numerical algorithm which differs from a standard Lagrangian finite-difference technique only in the approximations to the spatial derivatives.

2.3. *One-Dimensional SPH Equations*

In one dimension, the SPH expression for conservation of mass becomes

$$\dot{\rho}^I = -\sum_{J=1}^{N} m^J (\dot{x}^I - \dot{x}^J) \frac{\partial W(u^{IJ})}{\partial x^J}, \tag{2.8}$$

where the expanded form of $\nabla \cdot V$ from Eq. (2.6) is used in order to avoid density difficulties at the boundaries [5]. The expression for conservation of momentum is

$$\ddot{x}^I = -\sum_{J=1}^{N} m^J \left(\frac{\sigma^J}{\rho^I \rho^J} + \Pi^{IJ} \right) \frac{\partial W(u^{IJ})}{\partial x^J}. \tag{2.9}$$

In the above expressions $\dot{x}$ is the velocity, the interparticle distance is

$$u^{IJ} = |x^I - x^J|, \tag{2.10}$$

and Π^{IJ} is the artificial viscosity in the form proposed by Monaghan [11]. The dependence of the kernel function on the smoothing length has not been explicitly included in these equations.

Although many authors use a symmetric form [3] of the equation of motion (conservation of momentum) in order to ensure exact momentum conservation, the asymmetric form has been used here for simplicity. In any event, it should be noted that under the simplifying assumptions which will be made during the course of the stability analysis the asymmetric and the symmetric forms reduce to the same expression.

3. INSTABILITY CRITERION

A stability analysis of the SPH equations will be carried out which will result in a sufficient condition for instability. In order to reduce the algebraic complexity of the analysis, simplified forms of the equations are first obtained. A summary of the steps involved in the analysis will help to motivate the assumptions made in simplifying the equations.

3.1. *Stability Analysis Sketch*

The SPH equations will be subjected to a stability analysis of a type which was popularized by John von Neumann (1903–1957); the basic idea can be traced back to Jean Baptiste Joseph Fourier (1768–1830). A von Neumann stability analysis consists of the following steps [12]:

1. Obtain the equations of first variation, which describe the propagation of small perturbations in the original equations. This is done by applying perturbations of the form

$$x \to x + \delta x \tag{3.1}$$

to each of the variables, then subtracting the unperturbed equations, keeping only terms which are first order in δx. All unperturbed quantities in the equations are frozen; the coefficients of the perturbations are considered constants. The resulting equations are known as the perturbation propagation equations. It should be emphasized that the analysis is concerned with the behavior of small perturbations, so that linear terms are dominant and nonlinear terms can be neglected ($\delta^2 \ll \delta$ when $\delta \ll 1$). This is the reason that the perturbation equations are linearized and that nonlinear terms can be dropped in the initial process of simplifying the equations. This does not reduce the generality of the analysis, since it is the initial stability of the method that is of concern, not the behavior at late stages after significant unstable growth has occurred and nonlinear effects may contribute.

2. Perform a Fourier analysis of the perturbation propagation equations, which involves assuming a separation of variables solution of the form

$$\delta x(X, t) = \delta x(t) e^{ikX}, \tag{3.2}$$

where X is the Lagrangian coordinate and k is the wavenumber of the perturbation.

3. For the resulting system of equations, find the amplification matrix $\boldsymbol{A}$, defined by

$$\boldsymbol{U}^{n+1} = \boldsymbol{A}\boldsymbol{U}^n, \tag{3.3}$$

where $\boldsymbol{U}^{n+1}$ is the vector of values at the new time step, and $\boldsymbol{U}^n$ is the vector of values at the old time step. The eigenvalues of $\mathbf{A}$, which depend on the wavenumber of the perturbation, determine the stability of the system of equations. If the largest eigenvalue exceeds unity, the amplitude of the value vector increases exponentially with time.

3.2. *Simplified One-Dimensional SPH Equations*

The most critical step in performing a stability analysis of the SPH equations is the reduction of the general forms involving sums over neighbor particles to simpler forms which are amenable to stability analysis but still retain the stability properties of the general equations. All simplifying assumptions which have been made for purposes of the analysis have been computationally verified to satisfy this requirement by direct substitution into a numerical code. In fact, calculations suggest that the simplified equations are more stable than the general forms.

If it is assumed that the smoothing length is equal to the initial interparticle distance, then nearest neighbors contribute to the particle sums, while next-nearest neighbors located a distance $2h$ away do not, since both the kernel function and its derivative are zero for $u^{IJ} \geq 2h$. Although the analysis will be generalized in Section 5 to include an arbitrary number of neighbors and an arbitrary ratio of smoothing length to particle spacing, for the present only nearest neighbors are considered. Equations (2.8) and (2.9) then reduce to

$$\begin{aligned}\dot{\rho}^I = -m[&(\dot{x}^I - \dot{x}^{I+1})W'(u^{I,I+1}) \\ &- (\dot{x}^I - \dot{x}^{I-1})W'(u^{I,I-1})]\end{aligned} \tag{3.4}$$

and

$$\begin{aligned}\ddot{x}^I = -m\Bigg[&\left(\frac{\sigma^{I+1}}{\rho^I\rho^{I+1}} + \Pi^{I,I+1}\right)W'(u^{I,I+1}) \\ &-\left(\frac{\sigma^{I-1}}{\rho^I\rho^{I-1}} + \Pi^{I,I-1}\right)W'(u^{I,I-1})\Bigg],\end{aligned} \tag{3.5}$$

where it has been assumed that the particles have been numbered in order of increasing position, x, so that $I - 1$ is the index of the nearest neighbor in the negative direction, while $I + 1$ is the index of the nearest neighbor in the positive direction. In writing these equations use has been made of the fact that in one dimension the derivative of the kernel function reduces to

$$\frac{\partial W(u^{IJ})}{\partial x^J} = \begin{cases} W'(u^{IJ}), & x^J > x^I \\ -W'(u^{IJ}), & x^J < x^I, \end{cases} \tag{3.6}$$

where the prime on W refers to the derivative with respect to the argument. In one dimension, W has dimensions of length^{-1}, while the mass, m, should be interpreted as mass per unit area, with the cross-sectional area numerically equal to one. The dimensions of W' are thus length^{-2}.

While it is possible to perform a stability analysis on Eqs. (3.4) and (3.5), the algebra becomes quite tedious, and clarity dictates further simplification of the equations before proceeding. If the densities in the denominators of Eq. (3.5) are taken to be constant for small perturbations, then

$$\begin{aligned}\ddot{x}^I = -\frac{m}{\rho^2}[&(\sigma^{I+1} + Q^{I,I+1})W'(u^{I,I+1}) \\ &- (\sigma^{I-1} + Q^{I,I-1})W'(u^{I,I-1})],\end{aligned} \tag{3.7}$$

where

$$Q^{I,I+1} = \rho^2\Pi^{I,I+1}. \tag{3.8}$$

Time derivatives will be approximated by centered-difference expressions, so that an equation of the form

$$\frac{df}{dt} = g \tag{3.9}$$

will become

$$\frac{f^{n+1/2} - f^{n-1/2}}{\Delta t} = g^n, \tag{3.10}$$

where the superscripts involving n denote the time at which the quantity is evaluated.

The one-dimensional SPH equation of motion thus becomes

$$\dot{x}^{l,n+1/2} - \dot{x}^{l,n-1/2} = -\frac{m\Delta t}{\rho^2}(T^{l+1}W'^{\,l+1/2} - T^{l-1}W'^{\,l-1/2})^n, \tag{3.11}$$

where

$$W'^{\,l+1/2} = W'(u^{l,l+1}), \tag{3.12}$$

the total stress, T, is given by

$$T^{l+1} = \sigma^{l+1} + Q^{l+1/2}, \tag{3.13}$$

and the linear term in the SPH viscosity [11] reduces in one dimension to

$$\begin{aligned} Q^{l+1/2} = Q^{l,l+1} &= \rho^2 \Pi^{l,l+1} = \alpha' \rho c(\dot{x}^{l+1} - \dot{x}^l) \\ &= \alpha(\dot{x}^{l+1} - \dot{x}^l), \end{aligned} \tag{3.14}$$

where α' is the original dimensionless coefficient [11] and additional constants have been included in the dimensional constant α. The quadratic term in the viscosity need not be considered, since it will be linearized in the perturbation propagation equations and the linear term is dominant for small perturbations in any event.

The only density dependence in Eq. (3.11) comes from the dependence of the stress, σ, on density. A linear dependence of stress on strain (Hooke's law) is described by the relation

$$\sigma = -K\eta = \rho_0 c^2\left(1 - \frac{\rho_0}{\rho}\right), \tag{3.15}$$

where $K = \rho_0 c^2$ is the bulk modulus, η is the volume strain, c is the sound speed, and stress is taken as negative in compression. Rather than using the continuity equation (conservation of mass) to find the strain, it can be noted that in one dimension, the volume associated with an interpolation point is determined by the positions that are half-way between the point and its neighbors to the left and right. The density can thus be determined from

$$\rho^l = \frac{2m}{x^{l+1} - x^{l-1}}. \tag{3.16}$$

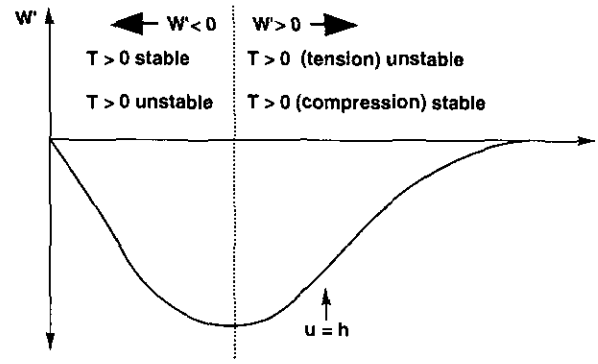

FIG. 3.1. Stability regimes for the cubic B-spline kernel.

Therefore, the stress can be expressed in terms of the particle positions by

$$\sigma^l = -K\left[1 - \frac{\rho_0}{2m}(x^{l+1} - x^{l-1})\right]. \tag{3.17}$$

Calculations using this simplified relation show that it produces solutions that are consistent with those provided by the continuity equation, and in fact it possesses smaller growth rates in unstable regimes. The only variables in Eq. (3.11) are thus velocity and position, which are related by

$$x^{l,n+1} = x^{l,n} + \Delta t \dot{x}^{l,n+1/2}. \tag{3.18}$$

Equations (3.11) and (3.18) constitute the simplified SPH equations to be analyzed for stability.

3.3. *Results*

The algebraic details of the stability analysis are given in Appendix A. The shortest wavelength, $\lambda_{\min}$, capable of being resolved by the discrete system is twice the particle spacing. The results show that at $\lambda_{\min}$, a sufficient condition for unstable growth is

$$W''T > 0, \tag{3.19}$$

where W'' is the second derivative of W with respect to its argument and is thus the slope of W'. The convention which is used throughout is that the stress T is negative in compression and positive in tension. The instability condition is independent of the artificial viscosity coefficients and the form of the kernel function. There are no stress or strain thresholds for the onset of the instability. The condition involves only the sign of the product of the total stress times the second derivative of the kernel function.

Figure 3.1 schematically summarizes the stability regimes for the specific case of the cubic B-spline kernel. If the slope of the derivative of the kernel function is positive, the method

is unstable in tension and stable in compression. If the slope is negative, it is unstable in compression and stable in tension. The derivative of the cubic B-spline kernel has its minimum value at $u = 2/3h$. In the standard configuration in which the particle spacing is equal to the smoothing length, the nearest-neighbor particles are at $u = h$, and the next-nearest-neighbors are at $u = 2h$ and do not interact. Thus, the standard configuration is stable if the stress is compressive, but unstable if it is tensile.

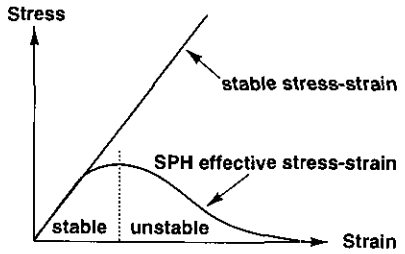

FIG. 4.1. Stable stress–strain relation and resulting SPH effective stress–strain relation after modification by $-W'$.

4. PHYSICS OF INSTABILITY GROWTH

While Eq. (3.19) provides a precise mathematical condition for instability, it does not provide a simple physical explanation of why SPH is unstable. In this section arguments are made to explain the reasons for the unstable behavior in terms of the form of the SPH equations. The mathematical models presented here are concerned with providing an intuitively understandable and easily communicable picture of the physics of the instability. This provides insight into the properties of the kernel function which are responsible for the instability and thus indicates possible means of removing the instability.

In one dimension, conservation of momentum is expressed by

$$\ddot{x} = \frac{\partial \sigma}{\rho_0 \partial X}, \tag{4.1}$$

where viscous stresses have been ignored, so that $T = \sigma$. In the discretization process associated with standard finite-difference methods, the partial derivatives are replaced by differences, so

$$\ddot{x} \approx \frac{\Delta \dot{x}}{\Delta t} = \frac{\Delta \sigma}{\rho_0 \Delta X}. \tag{4.2}$$

However, $\rho_0 \Delta X$ is just the mass, so the finite-difference equation of motion has the form

$$\ddot{x} \approx \frac{\Delta \sigma}{m} \propto \Delta \sigma. \tag{4.3}$$

However, Eq. (3.5) shows that the form of the SPH equation of motion is

$$\ddot{x} \propto \Delta(-\sigma W'), \tag{4.4}$$

where the difference operator Δ is a result of the sum over particles. Comparison of Eqs. (4.3) and (4.4) shows that in SPH the effective stress is proportional to $-\sigma W'$. Figure 4.1 shows that when a normal monotonically increasing stress–strain relation is multiplied by a function like $-W'$ which eventually goes to zero as particles separate, the resulting SPH effective stress–strain relation will contain regions where the effective stress decreases with increasing strain, producing a negative modulus and thus an imaginary sound speed. The stress–strain relation is clearly unstable in such a region, since changes in stress act to amplify, rather than reduce, changes in strain.

Note that Eq. (3.5) and Eq. (4.4) are independent of the numerical time integration algorithm, and thus the instability is not caused by the temporal difference scheme, but rather by the effective SPH stress containing regions with imaginary sound speeds. This point can be further illustrated by considering the one-dimensional wave equation

$$\frac{\partial^2 u}{\partial t^2} = c^2 \frac{\partial^2 u}{\partial x^2}, \tag{4.5}$$

where u is displacement and c is the sound speed, $\sqrt{dP/d\rho}$. Perform an elementary Fourier analysis by substituting into this equation a solution of the form

$$u = e^{ikx+gt}. \tag{4.6}$$

The resulting growth factors are given by

$$g = \pm\sqrt{-c^2k^2}. \tag{4.7}$$

Thus, if $c^2 > 0$, the growth factors are imaginary and solutions are bounded, while if $c^2 < 0$, the growth factors are real, and the displacement increases exponentially in time. This result is a property of the differential equations and is not caused by any numerical solution technique.

The above analysis can be extended to show why the instability condition is independent of the artificial viscosity coefficients. The linear artificial viscosity term is related to the velocity gradient by

$$Q \propto \alpha \frac{\partial \dot{u}}{\partial x} = \alpha \frac{\partial^2 u}{\partial t \partial x}. \tag{4.8}$$

Since the acceleration due to the artificial viscosity is related to the gradient of the viscous stress, the wave equation becomes

$$\frac{\partial^2 u}{\partial t^2} = c^2 \frac{\partial^2 u}{\partial x^2} + \alpha \frac{\partial^3 u}{\partial t \partial x^2} \tag{4.9}$$

and the growth factors are given by

$$g = \frac{-\alpha k^2 \pm \sqrt{(\alpha k^2)^2 - 4c^2 k^2}}{2}. \tag{4.10}$$

If $c^2 < 0$, the growth factors are real and the displacement increases exponentially in time, regardless of the value of the artificial viscosity coefficient. Thus, artificial viscosity cannot stabilize the imaginary sound speed condition responsible for the SPH instability. The addition of quadratic viscosity terms will not help, since the quadratic viscosity term is only dominant in high gradient regions such as shock fronts, and the linear viscosity term dominates when gradients are small, such as during the initial growth of the instability.

The above discussion, while showing how the kernel function can introduce nonlinearities into the problem which can cause instabilities, seems to indicate that an unstable regime would not be entered until enough strain had accrued to cause the product of the equation-of-state stress times the kernel function to change slope. However, the instability criterion, Eq. (3.19), shows no thresholds. This is due to the fact that Eq. (4.4) does not include the frequency dependence of the stability analysis leading to Eq. (3.19).

Referring to the details of the stability analysis in Appendix A, it can be seen that Eq. (A.10), the perturbation propagation equation, has the form

$$\delta \ddot{x} = \frac{\Delta \delta \dot{x}}{\Delta t} \propto \Delta(\delta(-\sigma W')) = \Delta(-\sigma \delta W' - W' \delta \sigma), \tag{4.11}$$

where the coefficients of the perturbations are constants and, again, viscous stresses have been ignored, so that $T = \sigma$. However, when the frequency dependence of the perturbation is considered, as in Eqs. (A.24) to (A.27), it is found that at the shortest wavelength.

$$W' \delta \sigma = 0. \tag{4.12}$$

Thus, at $\lambda_{\min}$,

$$\delta \ddot{x} \propto -\sigma \Delta(\delta W'), \tag{4.13}$$

which is the equation of first variation of

$$\ddot{x} \propto -\sigma \Delta W'. \tag{4.14}$$

Comparison with Eq. (4.3) shows that at the minimum wavelength, the effective stress is just a constant multiple of the kernel function derivative, dependent only on the signed magnitude of the stress. Thus, as shown in Fig. 4.2, the effective stress is just an image of the kernel function.

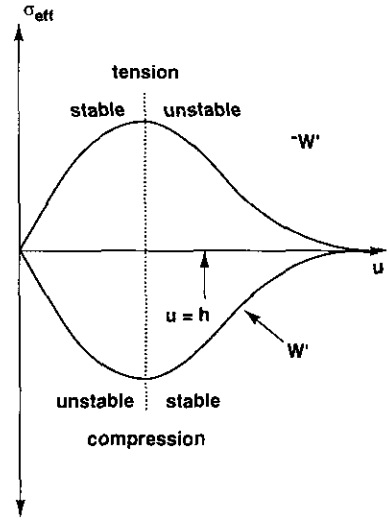

FIG. 4.2. Effective stress at the minimum wavelength.

If the stress is compressive, σ is negative and the effective stress is proportional to W'. When the slope of W' is positive, compressive stress decreases as particles separate and increases as particles approach, which is stable. When the slope of W' is negative, compressive stress increases as particles separate and decreases as particles approach, which is unstable.

If the stress is tensile, σ is positive and the effective stress is proportional to $-W'$. When the slope of $-W'$ is positive, tensile stress increases as particles separate and decreases as particles approach, which is stable. When the slope of $-W'$ is negative, tensile stress decreases as particles separate and increases as particles approach, which is unstable.

The above constitutes a lengthy statement of the condition expressed so concisely in Eq. (3.19), but it does give a physical interpretation of the instability condition. The normal situation in which the cubic B-spline kernel is used with nearest-neighbor particles located at $u = h$ is unstable in tension and stable in compression. However, it can be seen that whenever the slope of W' is not zero, either tension or compression will be unstable. This result is not caused by the numerical time integration algorithm, but is instead the result of the kernel approximation producing an effective stress with a negative modulus and, thus, imaginary sound speeds.

5. INSTABILITY CONDITION FOR AN ARBITRARY NUMBER OF NEIGHBORS

The stability criterion derived in Appendix A assumes that only nearest neighbors interact, in that it includes terms only at $I \pm 1$. However, having the analysis as a guide, it becomes clear that an extension to include an arbitrary number of neigh-

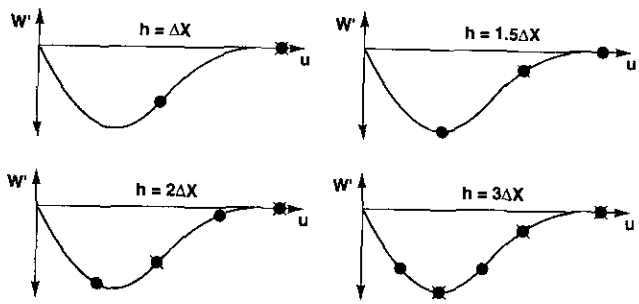

FIG. 5.1. Particle–kernel interactions for various smoothing lengths.

bors will result only in extra terms in the equations for particles at $I \pm 2$, $I \pm 3$, $I \pm 4$, etc. For instance, each term in Eq. (A.10) will be repeated with indices $I \pm 1$ changed to $I \pm 2$, then repeated again using $I \pm 3$, and so on. As these terms are carried forward they result in terms with different powers of E in Eq. (A.24). In these equations, the values of W' and W'' have been evaluated at u equal to the distance from particle I to particles at $I \pm 1$. These values will change for particles at $I \pm 2$, etc., but if it is still assumed that other quantities such as stress are the same at all particles, the generalized form of the instability criterion can easily be demonstrated to be

$$(W''^{I,I\pm1} + W''^{I,I+3} + W''^{I,I+5} + \cdots)\, T > 0. \tag{5.1}$$

Thus, it is just the sum of the values of W'' at all particles with odd separations from particle I falling within the smoothing length $2h$ which determines whether the system is stable in tension or compression. The particles at even separations, such as $I \pm 2$, $I \pm 4$, etc., do not contribute because they result in terms in Eq. (A.27) which contain $\cos 2l\pi - 1$, where l is an integer, while the odd particles result in terms which contain $\cos(2l + 1)\pi - 1$. Thus, various situations can result, as indicated in Fig. 5.1, depending on the relation of the smoothing length to the initial particle spacing. In this figure, the even particles which do not contribute have been crossed out. Note that for the cubic B-spline kernel, a smoothing length of $1.5\Delta X$ results in odd particles being located where the slope of W' is zero. This configuration is thus stable in one dimension for very small perturbations, but for larger perturbations the particles move to regions of nonzero slope and instability again results.

6. CONCLUSIONS

A stability analysis of the SPH algorithm has provided a simple criterion for the instability of the method which depends only on the sign of the product of the stress times the second derivative of the kernel function. There are no stress or strain thresholds for the onset of the instability. In standard SPH calculations using the cubic B-spline kernel the instability will normally only occur in tension. It is thus typically not a problem with equations of state that do not generate tensile stresses, which is the usual case in astrophysical applications; it will more frequently be encountered when SPH is extended to solid dynamics.

The instability criterion is independent of the viscosity coefficients and the instability cannot be removed by increasing the amount of artificial viscosity. However, the perturbation growth rate does depend on the stress level and the amount of artificial viscosity. Thus, whether or not effects of the instability are observed depends on the perturbation growth rate, the amplitude of the perturbations, and the amount of time the system remains in an unstable regime.

The instability is not caused by the time integration algorithm, but is due instead to a negative effective modulus (imaginary sound speed) resulting from the interaction of the kernel function with the constitutive relation. In other words, the instability is due to an effective stress which amplifies, rather than reduces, the applied strains. Although the effective modulus is frequency dependent, it is the highest frequency capable of being resolved by the discrete system, commonly called the noise frequency, which has the maximum growth. Thus particle-to-particle fluctuations which grow with time are the result of the instability. However, growth only continues so long as the particle spacings result in a stress state and a value of W'' which satisfy the instability criterion. Particles will thus tend to clump together in stable configurations, as has been previously observed [13, 14]. This clumping resembles fracture and fragmentation, but is in fact a numerical artifact.

Although the usual situation involving the cubic B-spline kernel with the smoothing length equal to the particle spacing is unstable in tension, instability in compression is also possible for different kernels. Various schemes suggest themselves to create a kernel coupled with a variable smoothing length so that the system is stable for the current sign of the stress. For instance, calculations verify that a kernel with W'' everywhere equal to zero is stable in all stress regimes. Unfortunately, such a kernel clearly cannot go to zero smoothly as the initial distance between particles increases, and this is one of the major requirements usually placed on the kernel in order to achieve compact support so that only particles within a limited range interact. Thus, local support results in at least some portion of the kernel function having W'' positive, which is unstable in tension. However, it seems unnecessary for the kernel to have regions where W'' is negative. A kernel modified in this way would eliminate the possibility of instability in compression. It remains the topic of further work to determine the required properties of the kernel function which maximize the accuracy and stability of the SPH method.

APPENDIX A

A.1. *Perturbation Propagation Equations*

In order to investigate the stability properties of Eqs. (3.11) and (3.18), we wish to consider the evolution of small perturba-

tions in the independent variables. That is, let positions be perturbed to

$$x^{I,n+1} \to x^{I,n+1} + \delta x^{I,n+1} \tag{A.1}$$

and velocities be perturbed to

$$\dot{x}^{I,n+1/2} \to \dot{x}^{I,n+1/2} + \delta\dot{x}^{I,n+1/2}. \tag{A.2}$$

Each position and velocity, regardless of its spatial and temporal index, will be replaced by a perturbed value as demonstrated in the above two equations. The equations describing the evolution of the perturbations are obtained by substituting the perturbed quantities into Eqs. (3.11) and (3.18), retaining only those terms that are linear in the perturbations and subtracting the original equations. All quantities other than the perturbations are assumed to be constant for purposes of the analysis.

The resulting expressions may be simplified by noting that the position and velocity perturbations of Eqs. (A.1) and (A.2) result in the following perturbations in the equation of state stress,

$$\sigma^{I+1,n} \to \sigma^{I+1,n} + \delta\sigma^{I+1,n}, \tag{A.3}$$

the viscous stress,

$$Q^{I+1/2,n} \to Q^{I+1/2,n} + \delta Q^{I+1/2,n}, \tag{A.4}$$

and the kernel function derivative,

$$W'^{I+1/2,n} \to W'^{I+1/2,n} + \delta W'^{I+1/2,n}, \tag{A.5}$$

where

$$\delta\sigma^{I+1,n} = \frac{\rho_0 K}{2m}(\delta x^{I+2,n} - \delta x^{I,n}), \tag{A.6}$$

$$\delta Q^{I+1/2,n} = \alpha(\delta\dot{x}^{I+1,n-1/2} - \delta\dot{x}^{I,n-1/2}), \tag{A.7}$$

$$\delta W'^{I+1/2,n} = W''^{I+1/2,n}(\delta x^{I+1,n} - \delta x^{I,n}). \tag{A.8}$$

The last equation follows from a first-order Taylor series expansion of W' and is independent of the form of the kernel function. W'' is the second derivative of W with respect to its argument and is thus the slope of W'.

Using the above notation, the perturbed form of Eq. (3.11) becomes

$$\begin{aligned}
&\dot{x}^{I,n+1/2} + \delta\dot{x}^{I,n+1/2} - \dot{x}^{I,n-1/2} - \delta\dot{x}^{I,n-1/2} \\
&= -\frac{m\Delta t}{\rho^2}[(\sigma^{I+1,n} + Q^{I+1/2,n} + \delta\sigma^{I+1,n} + \delta Q^{I+1/2,n}) \\
&\quad (W'^{I+1/2,n} + \delta W'^{I+1/2,n}) \\
&\quad - (\sigma^{I-1,n} + Q^{I-1/2,n} + \delta\sigma^{I-1,n} + \delta Q^{I-1/2,n}) \\
&\quad (W'^{I-1/2,n} + \delta W'^{I-1/2,n})]
\end{aligned} \tag{A.9}$$

The linearized form of this equation, after dropping the higher-than-linear terms in the perturbations and subtracting the original equation, becomes

$$\begin{aligned}
\delta\dot{x}^{I,n+1/2} - \delta\dot{x}^{I,n-1/2} = -\frac{m\Delta t}{\rho^2}&(T^{I+1,n}\delta W'^{I+1/2,n} - T^{I-1,n}\delta W'^{I-1/2,n} \\
&+ W'^{I+1/2,n}\delta\sigma^{I+1,n} - W'^{I-1/2,n}\delta\sigma^{I-1,n} \\
&+ W'^{I+1/2,n}\delta Q^{I+1/2,n} - W'^{I-1/2,n}\delta Q^{I-1/2,n})
\end{aligned} \tag{A.10}$$

where the total stress, T, is given by

$$T^{I+1,n} = \sigma^{I+1,n} + Q^{I+1/2,n}. \tag{A.11}$$

This result can easily be verified by noting that each cross-product produces surviving terms which consist of the constants in the first term times the perturbations in the second, plus the constants in the second term times the perturbations in the first. Substituting Eq. (A.6), Eq. (A.7), and Eq. (A.8) into Eq. (A.10) yields

$$\begin{aligned}
\delta\dot{x}^{I,n+1/2} = \delta\dot{x}^{I,n-1/2} &- \frac{m\Delta t}{\rho^2}\Big\{W''^{I+1/2,n}T^{I+1,n}(\delta x^{I+1,n} - \delta x^{I,n}) \\
&- W''^{I-1/2,n}T^{I-1,n}(\delta x^{I,n} - \delta x^{I-1,n}) \\
&+ \frac{\rho_0 K}{2m}[W'^{I+1/2,n}(\delta x^{I+2,n} - \delta x^{I,n}) \\
&- W'^{I-1/2,n}(\delta x^{I,n} - \delta x^{I-2,n})] \\
&+ \alpha[W'^{I+1/2,n}(\delta\dot{x}^{I+1,n-1/2} - \delta\dot{x}^{I,n-1/2}) \\
&- W'^{I-1/2,n}(\delta\dot{x}^{I,n-1/2} - \delta\dot{x}^{I-1,n-1/2})]\Big\}
\end{aligned} \tag{A.12}$$

and

$$\delta x^{I,n+1} = \delta x^{I,n} + \Delta t\,\delta\dot{x}^{I,n+1/2}. \tag{A.13}$$

These equations describe the propagation of small perturbations in the velocity and position.

A.2. *Fourier Decomposition*

A Fourier analysis is now performed which involves the assumption of a separation of spatial and temporal variables of the form

$$\delta x^{I,n} = \delta x^n E^I, \tag{A.14}$$

$$\delta\dot{x}^{I,n-1/2} = \delta\dot{x}^{n-1/2}E^I, \tag{A.15}$$

where

$$E^I = (e^{ik\Delta X})^I = \cos(Ik\Delta X) + i\sin(Ik\Delta X) \tag{A.16}$$

describes the spatial variation of the perturbed quantities. In this expression X is the initial, or Lagrangian, coordinate, so that ΔX is the initial uniform spacing between particles and E^I represents E being raised to the power I, rather than an index. The position of particle I at time zero is thus given by

$$x^I = I\Delta X. \tag{A.17}$$

The perturbation is assumed to be periodic with wavenumber, k, which is the circular inverse of the perturbation wavelength, λ, so that

$$k\Delta X = \frac{2\pi}{\lambda}\Delta X. \tag{A.18}$$

Substituting the separated variable solutions into the perturbation propagation equations and dividing by E^I yields

$$\begin{aligned}\delta\dot{x}^{n+1/2} = \delta\dot{x}^{n-1/2} &- \frac{m\Delta t}{\rho^2}\Big\{W''^{I+1/2,n}T^{I+1,n}(E-1)\\ &- W''^{I-1/2,n}T^{I-1,n}(1-E^{-1})\\ &+ \frac{\rho_0 K}{2m}[W'^{I+1/2,n}(E^2-1)\\ &- W'^{I-1/2,n}(1-E^{-2})]\Big\}\delta x^n\\ &- \frac{\alpha m\Delta t}{\rho^2}[W'^{I+1/2,n}(E-1)\\ &- W'^{I-1/2,n}(1-E^{-1})]\delta\dot{x}^{n-1/2}\end{aligned} \tag{A.19}$$

and

$$\delta x^{n+1} = \delta x^n + \Delta t\,\delta\dot{x}^{n+1/2}. \tag{A.20}$$

These expressions can be simplified by considering the case of a uniform initial state, so that

$$W'^{I+1/2,n} = W'^{I-1/2,n} = W', \tag{A.21}$$

$$W''^{I+1/2,n} = W''^{I-1/2,n} = W'', \tag{A.22}$$

and

$$T^{I+1,n} = T^{I-1,n} = T. \tag{A.23}$$

Equation (A.19) then becomes

$$\begin{aligned}\delta\dot{x}^{n+1/2} = \delta\dot{x}^{n-1/2} &- \frac{m\Delta t}{\rho^2}\Big[W''T(E+E^{-1}-2)\\ &+ \frac{\rho_0 KW'}{2m}(E^2+E^{-2}-2)\Big]\delta x^n\\ &- \frac{\alpha mW'\Delta t}{\rho^2}(E+E^{-1}-2)\delta\dot{x}^{n-1/2}.\end{aligned} \tag{A.24}$$

However,

$$E + E^{-1} - 2 = 2\left(\cos\frac{2\pi\Delta X}{\lambda} - 1\right), \tag{A.25}$$

while

$$E^2 + E^{-2} - 2 = 2\left(\cos\frac{4\pi\Delta X}{\lambda} - 1\right). \tag{A.26}$$

Equation (A.24) thus becomes

$$\begin{aligned}\delta\dot{x}^{I,n+1/2} = \delta\dot{x}^{I,n-1/2} &- \frac{2m\Delta t}{\rho^2}\left[W''T\left(\cos\frac{2\pi\Delta X}{\lambda} - 1\right)\right.\\ &\left.+ \frac{\rho_0 KW'}{2m}\left(\cos\frac{4\pi\Delta X}{\lambda} - 1\right)\right]\delta x^n\\ &- \frac{2\alpha mW'\Delta t}{\rho^2}\left(\cos\frac{2\pi\Delta X}{\lambda} - 1\right)\delta\dot{x}^{I,n-1/2}.\end{aligned} \tag{A.27}$$

The first term in brackets multiplying δx^n involves kernel variations at constant stress, while the second term in brackets multiplying δx^n involves stress variations at a constant value of the kernel. The term multiplying $\delta\dot{x}^{I,n-1/2}$ involves the artificial viscosity. The shortest wavelength perturbation which can be resolved by the discrete system is

$$\lambda_{\min} = 2\Delta X. \tag{A.28}$$

At this wavelength the term involving stress variations goes to zero, so that the equation of state stress has no effect on the propagation of perturbations at the shortest wavelength.

A.3. *Amplification Matrix Eigenvalues*

The perturbation propagation equations can be rewritten in the form

$$\delta\dot{x}^{n+1/2} = (1 - r\Delta t)\delta\dot{x}^{n-1/2} + s\Delta t\,\delta x^n \tag{A.29}$$

and

$$-\Delta t\,\delta\dot{x}^{n+1/2} + \delta x^{n+1} = \delta x^n, \tag{A.30}$$

where

$$r = \frac{2\alpha m W'}{\rho^2}\left(\cos\frac{2\pi\Delta X}{\lambda} - 1\right) \tag{A.31}$$

and

$$s = -\frac{2m}{\rho^2}\left[W''T\left(\cos\frac{2\pi\Delta X}{\lambda} - 1\right) + \frac{\rho_0 K W'}{2m}\left(\cos\frac{4\pi\Delta X}{\lambda} - 1\right)\right]. \tag{A.32}$$

Rewriting these equations in matrix format yields

$$\boldsymbol{L}\boldsymbol{U}^{n+1} = \boldsymbol{R}\boldsymbol{U}^n, \tag{A.33}$$

where the vector of new velocities and positions is

$$\boldsymbol{U}^{n+1} = \begin{bmatrix} \delta\dot{x}^{n+1/2} \\ \delta x^{n+1} \end{bmatrix}, \tag{A.34}$$

the vector of old velocities and positions is

$$\boldsymbol{U}^n = \begin{bmatrix} \delta\dot{x}^{n-1/2} \\ \delta x^n \end{bmatrix}, \tag{A.35}$$

and

$$\boldsymbol{L} = \begin{bmatrix} 1 & 0 \\ -\Delta t & 1 \end{bmatrix}, \tag{A.36}$$

$$\boldsymbol{R} = \begin{bmatrix} (1 - r\Delta t) & s\Delta t \\ 0 & 1 \end{bmatrix}. \tag{A.37}$$

The stability of this set of equations is determined by the eigenvalues of the amplification matrix $\boldsymbol{A}$, where

$$\boldsymbol{U}^{n+1} = \boldsymbol{A}\boldsymbol{U}^n. \tag{A.38}$$

Comparison with Eq. (A.33) shows that

$$\boldsymbol{A} = \boldsymbol{L}^{-1}\boldsymbol{R}. \tag{A.39}$$

Determination of the eigenvalues of $\boldsymbol{A}$ can be simplified by noting that

$$|\boldsymbol{A} - \hat{\lambda}\boldsymbol{I}| = 0 \Leftrightarrow |\boldsymbol{L}|\,|\boldsymbol{A} - \hat{\lambda}\boldsymbol{I}| = |\boldsymbol{R} - \hat{\lambda}\boldsymbol{L}| = 0. \tag{A.40}$$

Thus, an equivalent procedure is to find the eigenvalues of

$$\boldsymbol{R} - \hat{\lambda}\boldsymbol{L} = \begin{bmatrix} (1 - r\Delta t - \hat{\lambda}) & s\Delta t \\ \hat{\lambda}\Delta t & 1 - \hat{\lambda} \end{bmatrix}. \tag{A.41}$$

The resulting eigenvalue equation is

$$\hat{\lambda}^2 + (r\Delta t - s\Delta t^2 - 2)\hat{\lambda} + 1 - r\Delta t = 0. \tag{A.42}$$

A.4. *Instability Condition*

The system is unstable, which is to say that values will grow exponentially, if the largest value of $\hat{\lambda}$ which results from the solution of Eq. (A.42) exceeds unity. Determination of stability is simplified by writing the eigenvalue equation in the form

$$\hat{\lambda}^2 - 2B\hat{\lambda} + C = 0, \tag{A.43}$$

where

$$B = 1 + \theta, \tag{A.44}$$

$$\theta = \frac{s\Delta t^2 - r\Delta t}{2}, \tag{A.45}$$

$$C = 1 - r\Delta t. \tag{A.46}$$

The value of the maximum eigenvalue depends on the value of the discriminant D, where

$$D = B^2 - C, \tag{A.47}$$

so that the eigenvalues are given by

$$\hat{\lambda} = B \pm D^{1/2}. \tag{A.48}$$

There are several cases to consider based on the sign of D and the magnitude of B, but in the current analysis all cases reduce to the statement that

$$D > 0 \tag{A.49}$$

is a sufficient condition for instability [15]. Combining Eqs. (A.44) to (A.47) yields

$$D = s\Delta t^2 + \theta^2, \tag{A.50}$$

so a sufficient condition for instability is

$$s > 0. \tag{A.51}$$

Note that the viscosity coefficient α is contained only in the

constant r, so viscosity cannot stabilize the system if Eq. (A.51) is satisfied.

At $\lambda_{\min}$, Eqs. (A.28) and (A.32) show that

$$s = \frac{4mW''T}{\rho^2}. \tag{A.52}$$

Therefore, a sufficient condition for unstable growth of the shortest wavelength (twice the particle spacing) is

$$W''T > 0, \tag{A.53}$$

where T is negative in compression and positive in tension. On the other hand, if

$$W''T < 0, \tag{A.54}$$

the system is conditionally stable, which means that the time step must be limited in order to achieve stability.

REFERENCES

1. L. B. Lucy, *Astrophys. J.* **82,** 1013 (1977).
2. R. A. Gingold and J. J. Monaghan, *J. Comput. Phys.* **46,** 429 (1982).
3. J. J. Monaghan, *SIAM J. Sci. Stat. Comput.* **3,** 422 (1982).
4. J. J. Monaghan, *Comput. Phys. Rep.* **3,** 71 (1985).
5. J. J. Monaghan, *Comput. Phys. Commun.* **48,** 89 (1988).
6. L. D. Cloutman, Lawrence Livermore National Laboratory Report UCRL-ID-103698, 1990.
7. L. D. Cloutman, in *Proceedings of The NEXT Free-Lagrange Conference, Jackson Lake Lodge, Moran, Wyoming, June* 3–7, 1990.
8. W. Benz, in *The Numerical Modeling of Stellar Pulsation,* edited by J. R. Buchler (Kluwer, Dordrecht, 1990), p. 269.
9. D. S. Balsara, *J. Comput. Phys.* **114,** No. 2 (1994).
10. R. D. Richtmyer and K. W. Morton, *Difference Methods for Initial Value Problems* (Interscience, New York, 1967), p. 295.
11. J. J. Monaghan and R. A. Gingold, *J. Comput. Phys.* **52,** 374 (1983).
12. G. G. O-Brien, M. A. Hyman, and S. Kaplan, *J. Math. Phys.* **29,** 223 (1951).
13. M. Schussler and D. Schmitt, *Astron. Astrophys.* **97,** 373 (1981).
14. P. A. Thomas and H. M. P. Couchman, *Mon. Not. R. Astron. Soc.* **257,** 11 (1992).
15. D. L. Hicks, *Math. Comput.* **32,** 1123 (1978).